High-pressure electrochemistry: a new frontier in decarbonization

High-pressure electrochemistry is an emerging area with significant promise for commercializing green chemicals. However, little is known about the underlying theories and practices in implementing high-pressure electrochemical reactors. Electrochemical synthesis at high pressures can increase the operating current density and reduce the cell potential, which would decrease the CapEx and OpEx costs, respectively, and thereby reduce barriers to industrial-scale deployment. In this perspective, we provide the fundamental theories of high-pressure electrochemistry and discuss how pressure affects the activity, selectivity, stability, and energy efficiency of reactions.

Image designed and illustrated by Crystal Price, Meenesh R Singh, and Joseph A. Gauthier

ROYAL SOCIETY OF CHEMISTRY

rsc.li/EESCatalysis

Check for updates

High-pressure electrochemistry: a new frontier in decarbonization†

Nishithan C. Kani, [ID] [a] Samuel Olusegun,[b] Rohit Chauhan,[a] Joseph A. Gauthier*[b] and Meenesh R. Singh [ID] *[a]

The chemical manufacturing of commodity chemicals, responsible for approximately 24% of global carbon emissions, poses a critical environmental challenge. With escalating demand due to economic development, urgent decarbonization strategies are imperative. Traditional electrochemical synthesis encounters hindrances, especially mass transfer limitations at relevant current densities, primarily attributed to gas phase reactants and products. In this Perspective, we explore the viability of high-pressure electrochemistry as a transformative solution. Our analysis reveals that applying pressure can overcome mass transfer limitations, enhance selectivity, and improve overall activity, all while minimizing energy consumption and capital expenditure for distributed production processes. We shed light on the influence of pressure on Pourbaix diagrams, electric double layer, electrolyte activity, conductivity, electrostriction-enhanced selectivities, catalyst activity, and stability. Additionally, insights are provided into the design and operation of existing reactors and tools for high-pressure electrochemistry, along with the imperative for future fundamental studies. In the context of decentralized production, we argue that the marginal differential capital costs associated with high-pressure reactors become inconsequential. Ultimately, our work seeks to pave the way for the decarbonization of the chemical industry by establishing innovative pathways for the electrochemical synthesis of commodity chemicals, presenting high-pressure electrochemical synthesis as a potential paradigm shift in this transformative journey.

Broader context

High-pressure electrochemistry is an emerging area with significant promise for commercializing green chemicals. However, little is known about the underlying theories and practices in implementing high-pressure electrochemical reactors. Electrochemical synthesis at high pressures can increase the operating current density and reduce the cell potential, which would decrease the CapEx and OpEx costs, respectively, and thereby reduce barriers to industrial-scale deployment. We review the fundamental theories of high-pressure electrochemistry and discuss how pressure affects the activity, selectivity, stability, and energy efficiency of reactions. We also explore the designs of reactors for synthesis and *in situ* characterization studies and the economics of high-pressure electrochemical synthesis.

1. Introduction

The steady increase in anthropogenic greenhouse gas (GHG) emissions has driven decarbonization needs for energy and chemical technologies. To achieve the net-zero carbon emissions target globally by the end of the 21st century,[1,2] it is

essential to develop and deploy net-zero and net-negative carbon technologies across various sectors. For instance, the decarbonization of power generation necessitates the utilization of solar, wind, and hydropower in conjunction with stable energy storage systems; the decarbonization of transportation can be achieved with electric vehicles concomitant with decarbonization of power generation; and the decarbonization of buildings can be done by implementing heat pumps and carbon-negative concrete. However, much-needed efforts towards decarbonizing chemical manufacturing are still lacking on a large scale. As a result, industrial manufacture of commodity chemicals is one of the most significant contributors to global GHG emissions, and it is predicted to rise from the demand for

[a] *Department of Chemical Engineering, University of Illinois Chicago, Chicago, IL 60607, USA*

[b] *Department of Chemical Engineering, Texas Tech University, Lubbock, TX 79409, USA. E-mail: mrsingh@uic.edu, joe.gauthier@ttu.edu*

commodities driven by economic development.[3] Combustion of fossil fuels, both for heating needs and for production of feedstocks (*e.g.*, H_2 from steam methane reforming and water gas shift reactions), are two significant sources of GHG emissions in producing commodity chemicals.

Decarbonization of chemical manufacturing is projected to follow two pathways. First, emissions can be mitigated by capturing emitted CO_2 and sequestration or valorization into value-added chemicals (CO, C_2H_4, CH_3OH, *etc.*). The second approach consists of avoiding the generation of CO_2 or other greenhouse gases in the first place. In particular, the second pathway can be achieved in several ways, including electrical heating, using green H_2 as a fuel for heating, and electrochemical synthesis of chemicals using renewable energy. A detailed review of the advantages and disadvantages of the technologies mentioned above is given in recent literature.[1,3] In brief, most of these technologies rely on photo/electrochemistry to capture and reduce GHG emissions by directly using renewably produced electrons. This work focuses on the electrochemical synthesis of chemicals using renewable energy. Specifically, we investigate the prospect of using high-pressure electrochemical processes for manufacturing commodity chemicals such as NH_3, C_2H_4, and CH_3OH while directly utilizing GHGs such as NO_x, CO_2, and CH_4.[4]

Electrochemical synthesis of the chemicals mentioned above is attractive, as the electric potential drives reactions, without extreme temperatures. In principle, this feature gives a distinct advantage of operating the reactor at ambient conditions using carbon-neutral electricity. Also, electrochemical processes provide opportunities to reduce downstream separation costs as a membrane separates the anode and cathode side products. The reactants used to produce the above-considered chemicals are typically gaseous, for example, N_2 from the air, captured CO_2, CO electrochemically synthesized from captured CO_2, excess CH_4 produced in natural gas extraction plants, NO_x from exhaust fumes, and H_2O.

Some examples of electrochemical conversion of gases include N_2 reduction to produce NH_3, CO_2/CO reduction to C_2H_4, and partial CH_4 oxidation to CH_3OH. The studies reported so far on the electrochemical synthesis of NH_3 from N_2 and H_2O under ambient conditions suffer from low yield (< -1 mA cm^{-2}),[5–7] though recent efforts in non-aqueous Li-mediated pathways show high selectivity.[8–10] As a result, it is difficult to attribute that produced NH_3 from the N_2 in reactant feed, not from adverse contaminants such as NO_x, NO_3^- and NO_2^-.[11–15] The process is very challenging due to the low solubility of N_2 in H_2O and the competing hydrogen evolution reaction (HER). In contrast, there has been considerable progress in the synthesis of C_2H_4 and CH_3OH electrochemically by reducing CO_2.[16–19] The challenges associated with the synthesis of these chemicals from CO_2 and CO are (1) tuning the selectivity of the products in a two electrode MEA based setup, as the product selectivity is strongly dependent on the applied potential; (2) low solubility of CO in H_2O; (3) competition with the HER. Finally, electrochemical oxidation of CH_4 to CH_3OH is desired as CH_3OH can be easily

stored and transported. Several studies[20,21] have reported the electrochemical oxidation of CH_4 to CH_3OH, and this process suffers from low solubility of CH_4 in H_2O, stability of the catalyst under highly oxidizing conditions, and the competing oxygen evolution reaction (OER). A common aspect of the above-mentioned processes is that they are synthesized from gas-phase reactants and suffer from mass transfer limitations due to the low solubility of the gases in aqueous media. Such challenges can be overcome by operating the reactors at higher pressures. While higher pressure will likely increase the reactor's capital cost, the operating cost to pressurize the reactor is low compared to increasing the reactors temperature.

Fundamental studies involving high-pressure electrochemistry have been reported as far back as the 1930s,[22–25] and high pressures are essential in studies involving hydrothermal systems, oceanographic analysis, and marine science.[26] High-pressure electrochemistry has been employed to get insights into the thermodynamics and kinetics of redox reactions at elevated pressures. Electrochemical properties such as redox potentials, diffusion, electron transfer rates, ion-solvent interactions, electrical double layer (EDL), *etc.*, depend on pressure.[26] Several studies have been reported in the literature that estimate the pressure dependence of these properties.[27–31] For example, a theoretical study by Guan *et al.*[32] predicts that metal superhydrides can be synthesized at high pressures simultaneously with an applied bias (known as the pressure-potential approach). Such a method extends the thermodynamic stability regime of super hydrides, which are challenging to form at ambient pressures. Similarly, electrochemical reduction of CO_2 at elevated pressures has been previously investigated.[33,34] At elevated pressures up to 30 atm, the overpotentials drop with a drastic improvement in the current densities and product selectivity.[33] The HER, a parasitic side reaction in electrochemical CO_2 reduction, was drastically suppressed around 30 bar, and 100% selectivity towards HCOOH was observed at 60 bar on Pb and In catalysts.[34] Ramdin *et al.*[35] used a high-pressure semicontinuous batch electrolyzer with Sn-based electrodes to reduce CO_2 to formates with 90% faradaic efficiency. Welch *et al.*[36] performed electrochemical CO_2 reduction in ionic liquids at high pressures and established a correlation between the volume expansion of ionic liquid and current densities. Electrochemical oxidation of CH_4 to CH_3OH at elevated pressures was investigated by Lee *et al.*[37] and Kim *et al.*,[38] who reported improved CH_3OH faradaic efficiencies with an increase in pressure. Synthesizing chemicals involving gas phase reactants electrochemically at high pressures would overcome the existing challenges, such as mass transfer limitations at ambient pressures. A brief summary of the literature comparisons is provided in the ESI.† In general, high-pressure electrochemistry and the effects of pressure are not well consolidated in the literature. This review provides a comprehensive and authoritative structure to the subject.

The purpose of high-pressure electrochemistry is (i) to improve the activity and selectivity of the redox reaction when the reactants are in the gas phase. Most reactions of interest,

such as N_2 reduction, N_2 oxidation, CO_2 reduction, and CH_4 oxidation, involve single gas phase reactants. By pressurizing, we mean pressurizing using the reactant gas; and (ii) to deliver the product gases at high pressure (e.g., high-pressure delivery of H_2 from PEM electrolyzers). In this case, the pressure of the anode/cathode chamber is regulated to the desired pressure by either accumulating pure product gases or by charging with a high-pressure sweep gas. The partial pressure will govern the activity of the product gases. Note that the pressure effects discussed in this work are related to the system's overall pressure, which will also be translated to the partial pressure effects. The electrochemical synthesis at high pressures can help increase operating current density and reduce cell potential, which would address a critical weakness inhibiting industrial-scale deployment. PEM electrolyzers are well-established and generally operate at high pressures. A brief description of the advantages of operating PEM electrolyzers at high pressures is provided in the ESI.† As shown below, the energy penalty associated with pressurizing a reactor is significantly lower than the energy required to heat it to extreme temperatures. Simultaneously, the overpotential required to make these chemicals at high pressures would be less than the ones at ambient pressures, thereby improving energy efficiency. The temperature significantly influences the reaction rates and thermodynamics in electrochemistry compared to pressure. Increasing the temperature can accelerate the reaction rates by providing more kinetic energy to the reactant molecules, increasing their collision frequency and enabling more successful collisions. However, in this review/perspective article, we focus only on the effect of pressure on the electrochemical systems, and we do not discuss in detail the role of temperature in improving performance.

This article reviews the fundamental theories of high-pressure electrochemistry and discusses how pressure affects the activity, selectivity, stability, and energy efficiency of reactions (see Fig. 1). We also explore the designs of reactors for synthesis and in situ characterization studies and the economics of high-pressure electrochemical synthesis.

2. Fundamentals of high-pressure electrochemical systems

Here, we discuss the role played by the pressure of gas phase reactants and products on the activity, selectivity, stability, and efficiency of electrochemical reactors.

2.1 Effect of pressure on thermodynamics

Energy requirement to pressurize reactors. The work done for an isentropic expansion of an ideal gas is given by,

$$W = \frac{P_1 V_1}{k-1}\left[1 - \left(\frac{P_1}{P_2}\right)^{\frac{1-k}{k}}\right] \quad (1)$$

where W is the work done (kJ), P_1 and P_2 are the pressures at states 1 and 2 (kPa), V_1 is the volume of the reactor (m^3), and k is the ratio of specific heat capacities of an ideal gas, i.e., C_p (specific heat capacity at constant pressure), and C_v (specific heat capacity at constant volume).

The work done to pressurize an ideal gas can be calculated from the above equation of isentropic expansion, which is normalized with respect to the number of moles of the ideal gas. Here, N_2 is taken as the model system. Fig. 2A shows the energy required to pressurize a reactor normalized with respect to the number of moles of gas as a function of the pressure. The energy required to pressurize a reactor to 10 bar is 60% of the energy required to pressurize a 300 bar reactor.

Electrochemical energy savings with increasing pressure. For a general redox reaction, a species O undergoing reduction at a cathode to species R is given by,

$$O + ne^- \rightleftharpoons R \quad (i)$$

The difference in equilibrium potentials at two different pressures P_1 and P_2 can be shown to be,

$$\Delta E = \frac{RT}{nF}\ln\left(\frac{P_2}{P_1}\right) \quad (2)$$

The difference in Gibb's free energy of the systems at pressures P_1 and P_2 can be obtained from the equilibrium
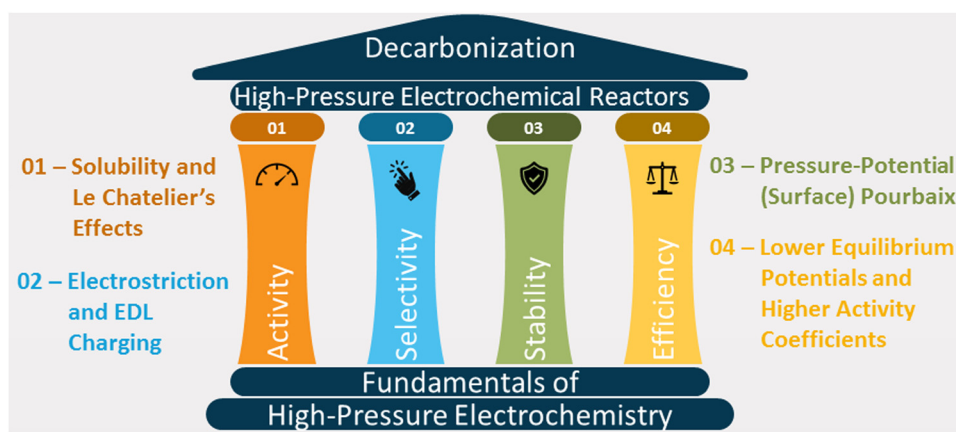

Fig. 1 Fundamental factors affecting activity, selectivity, stability, and energy efficiency of high-pressure electrochemical systems.
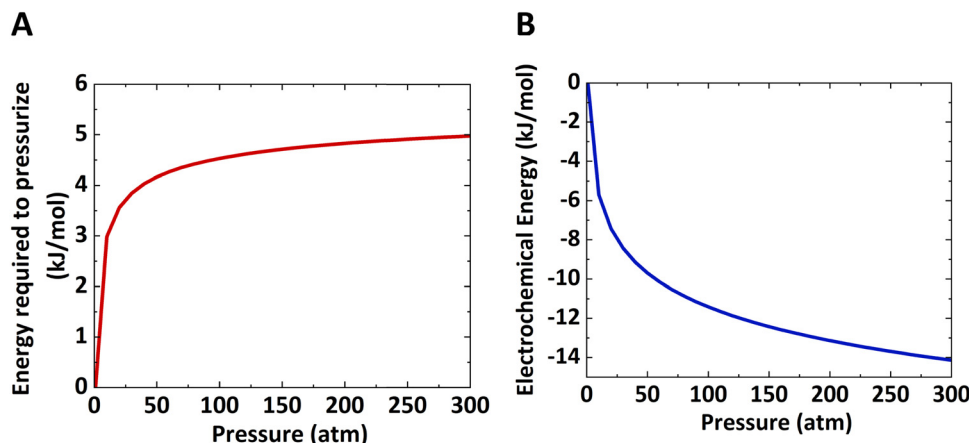
A

B

Fig. 2 Thermodynamic energy requirements: (A) energy required to pressurize a reactor as a function of pressure assuming isentropic expansion of an ideal gas. (B) Electrochemical energy reduction for any redox reaction as a function of pressure.

potential difference in eqn (2),

$$\Delta G = -RT \ln\left(\frac{P_2}{P_1}\right) \tag{3}$$

Fig. 2B shows that the electrochemical energy requirement decreases with increasing pressure. While the reduction in equilibrium potential depends on the number of electrons transferred per mole of the product (see eqn (2)), the free energy reduction does not depend on the type of redox reaction (see eqn (3)).

To summarize, the energy savings from the reduction in electrochemical potential are at least double the energy penalty for pressurizing the reactors. Therefore, the operating costs are lower for pressurized electrochemical reactors. However, the capital cost to build a thick-wall reactor to withstand high pressures will be higher than for a reactor operated at ambient pressure.

Selective shifts of redox lines in the pourbaix diagram at increasing pressure. The Pourbaix diagram of redox reactions is affected by changes in pressure. We calculated the Pourbaix diagrams using the Nernst equation (eqn (2)) for the electrode half-cell reactions considered in Table 1 at 1 bar and at 200 bars. A detailed description of the calculations is given in the ESI.† Tables 1 and 2 indicate the half-cell reactions and the overall reactions for the considered systems. Fig. 3 shows

Table 1 Half-cell reactions with their equilibrium potential (at 298.15 K, pH = 0 and P = 1 and 200 bar) for the considered systems

		Equilibrium potential (V vs. RHE), pH = 0	
Sr. No.	Half cell reaction	$P = 1$ bar	$P = 200$ bar
1	$N_2 + 6H^+ + 6e^- \rightarrow 2NH_3$	0.056	0.079
2	$CH_4 + H_2O \rightarrow CH_3OH + 2H^+ + 2e^-$	0.58	0.51
3	$2CO_2 + 12H^+ + 12e^- \rightarrow C_2H_4 + 4H_2O$	0.08	0.10
4	$2CO + 8H^+ + 8e^- \rightarrow C_2H_4 + 2H_2O$	0.17	0.20
5	$CO_2 + 6H^+ + 6e^- \rightarrow CH_3OH + H_2O$	0.03	0.05
6	$CO + 4H^+ + 4e^- \rightarrow CH_3OH$	0.08	0.11
7	$2H_2O \rightarrow O_2 + 4H^+ + 4e^-$	1.23	1.23
8	$2H^+ + 2e^- \rightarrow H_2$	0.00	0.00

Table 2 Overall reactions for the considered systems

S. no.	Overall reaction
1	$2N_2 + 6H_2O \rightarrow 4NH_3 + 3O_2$
2	$CH_4 + H_2O \rightarrow CH_3OH + H_2$
3	$2CO_2 + 2H_2O \rightarrow C_2H_4 + 3O_2$
4	$2CO + 2H_2O \rightarrow C_2H_4 + 2O_2$
5	$2CO_2 + 4H_2O \rightarrow 2CH_3OH + 3O_2$
6	$CO + 2H_2O \rightarrow CH_3OH + O_2$

the effect of pressure on the Pourbaix diagrams for different half-cell reactions.

With increasing pressure, the Pourbaix lines shift up for reduction reactions and shift down for oxidation reactions. In both half-cell reactions, the overpotential will decrease with increasing pressure. The shift in Pourbaix lines is not significant for reactions with a higher number of electron transfers, such as electrosynthesis of C_2H_4 from CO_2 and CO (< 0.05 V). The electrochemical reactions, such as CH_4 to CH_3OH, CO_2 to CO, CO_2 to HCOOH, etc., would be significantly improved with applied pressure.

Improved competitive binding of the reactant with increasing pressure. Beyond the energetic requirements of a process, pressure as an independent variable can also directly impact the binding energies of critical reaction intermediates. To demonstrate this utility, consider Fig. 4, which demonstrates a linear scaling relation between dinitrogen (N_2) binding (ΔE_{N_2}) and hydroxide binding (ΔE_{OH}) on various metals and rutile oxides at two different applied potentials at atmospheric pressure. The process under consideration here, as an example, is the electrochemical N_2 oxidation reaction (N_2OR). A significant consideration for this process is the competitive binding of N_2 with OER intermediates. An ideal catalyst for this process will bind N_2 more strongly than OER intermediates, given by catalysts below the dashed line. Simultaneously, N_2 must bind exergonically on the surface, with thermoneutral N_2 binding denoted by the solid black line. Thus, a region containing catalysts of interest is given by the region below both the
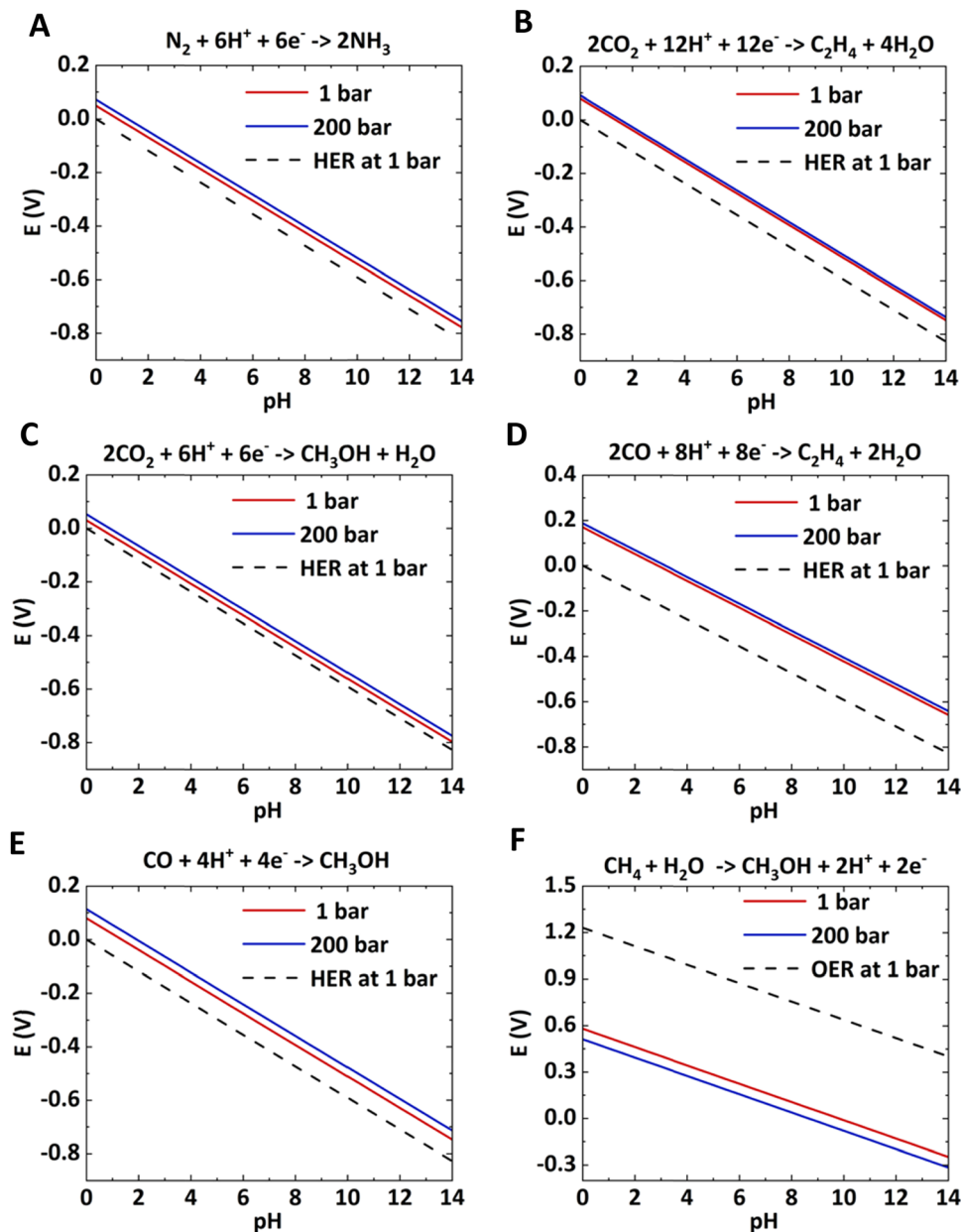
Fig. 3 Effect of pressure on the bulk Pourbaix diagram for different half–cell reactions.

dashed and solid black lines. Under relevant operating conditions (equilibrium potential of the N$_2$OR is $\sim$+1.3 V *vs.* RHE at 1 atm pressure), no catalysts in this pool showed the desired characteristics.

Note that the energetics reported here are (approximately) enthalpies. A standard procedure in estimating entropic effects (where pressure plays the most significant role) for binding (Gibbs free) energy calculations is two-fold: (i) for the adsorbed state, molecules are typically assumed to have only vibrational degrees of freedom, with the overall entropy described by the harmonic oscillator approximation. Note that this approximation has been explored extensively in the literature, with recent findings suggesting that, for small molecules on metal surfaces, the HO approximation provides an excellent

approximation for the entropy.[39–41] (ii) For the gas-phase state, typically, molecules are approximated using the ideal gas approximation, in which the translational component of the entropy depends on the logarithm of the pressure. Here, the *y*-axis of Fig. 4 represents the reaction,

$$N_{2(g)} + * \rightarrow N_2^* \tag{ii}$$

Given that the Gibbs free energy of the left-hand side of this equation is destabilized logarithmically with pressure, the dinitrogen binding energetics will become more favorable as N$_2$ pressure is increased (*i.e.*, red and purple lines will shift downwards), expanding the "region of interest" highlighted in panel (A).
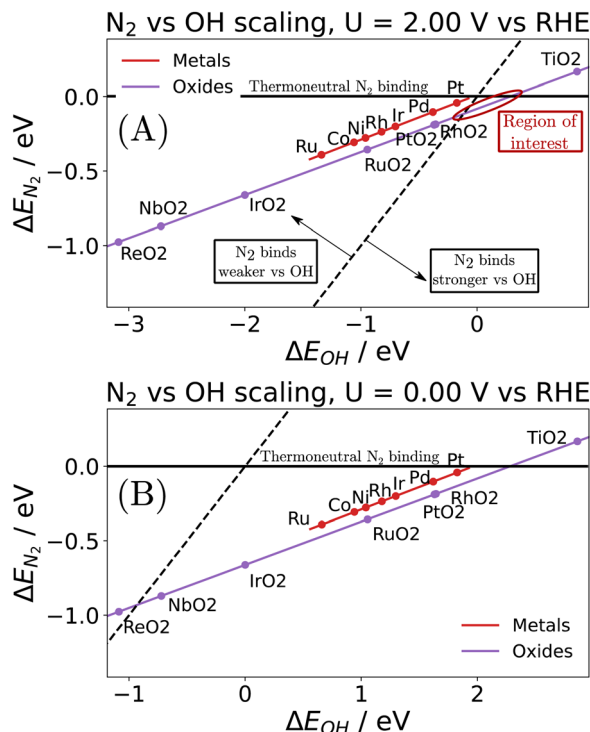
Fig. 4 Illustration of the scaling between N_2 binding and hydroxide binding on various metals and rutile oxides at an applied bias of (A) U = +2 V *vs.* RHE, and (B) U = 0.0 V *vs.* RHE. Note that N_2 binding is first order independent of potential, while hydroxide binding depends linearly on potential.

Although a complete exploration of the energetic landscape of the N_2OR has, to our knowledge, not yet been published, in Fig. 5, we illustrate a limiting potential OER volcano and a schematic N_2OR limiting potential volcano.

Here, the *y*-axis represents the negative theoretical limiting potential for the reaction of interest, while the *x*-axis represents the binding energy of atomic nitrogen, which is linearly correlated with the typical OER descriptor $\Delta E_O - \Delta E_{OH}$. Here, catalysts closer to the dashed black line are predicted to be more active for the given reaction. The schematic N_2OR volcano, based in part on the scaling lines from Fig. 4, shows that
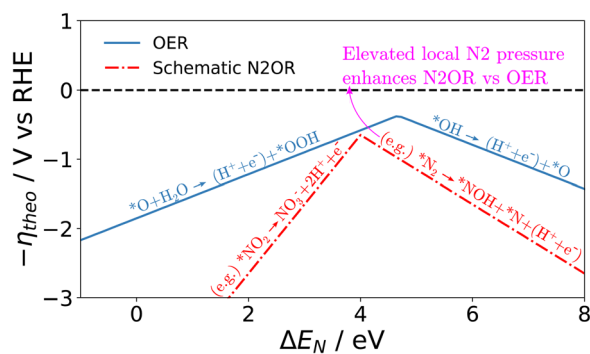

Fig. 5 Limiting potential volcanoes for the oxygen evolution reaction (OER) and dinitrogen oxidation reaction (N_2OR, schematic shown) with a common descriptor given as the binding energy of atomic nitrogen.

no catalyst will be more active towards the N_2OR than the competing OER. However, if one of the legs of the N_2OR volcano involves $N_{2(g)}$ as a reactant, elevated N_2 pressure will enhance the N_2OR, while having no effect on the OER. In our schematic N_2OR volcano, increasing the N_2 pressure effectively raises the right leg, shifting the peak to the right and potentially overcoming the OER-limiting potential volcano.

2.2 Effect of pressure on the reaction kinetics or current density

Generally, the kinetic rate of redox reactions increases with increasing the pressure of the reactant. This effect is primarily due to the higher solubility of dissolved gases and the lower equilibrium potential of redox reactions at elevated pressures.

Increasing solubility and deviation from Henry's law. The solubility of non-polar gases such as H_2, N_2, CH_4, and O_2 follows Henry's law over a wide range of pressures.[42] The mole fraction of dissolved gases increases almost linearly with increasing pressures up to 100 bar. Such linear trends may bend if the pressurized gases deviate from ideal gas behavior. For example, CO_2 solubility starts deviating from linear behavior from pressures exceeding 60 bar.[43] Another example is the gases that exist as a vapor (*e.g.*, H_2O). These vapor gases follow Henry's law only up to one-half to two-thirds of their saturation point. Such deviations from Henry's law directly affect the rate of redox reaction.

Reduction in equilibrium potential due to volume change. The kinetic rate or current density of the electrochemical reaction changes with increasing pressure as per Le Chatelier's principle, which states that at a constant temperature, the change in Gibb's free energy (ΔG°) with respect to pressure equals the standard volume change of the reaction.[44] This is denoted by the mathematical expression,

$$\left[\frac{\partial(\Delta G^\circ)}{\partial P}\right]_T = \Delta V^\circ \qquad (4)$$

where ΔV° is the standard volume change of the reaction, which is the difference between the sum of the standard molar volumes of the products and the sum of the standard molar volumes of the reactants. As per Le Chatelier's principle, the reaction that involves a net decrease in volume is favored by an increase in pressure and *vice versa*. The relationship between the standard potential of an electrochemical redox reaction and pressure is given by the equation,

$$\left[\frac{\partial(\Delta E^\circ)}{\partial P}\right]_T = -\frac{1}{nF}\Delta V^\circ \qquad (5)$$

The reaction will be favored by increasing the pressures if the activated complex has a smaller partial volume than the reactants. As per Le-Chatelier's principle, when the pressure of reactant gases such as N_2, CO_2, CO, and CH_4 is increased, they would favor the forward reaction as the reactions proceed by a net decrease in volume. At elevated pressures, the current densities of the products would be drastically higher than at ambient pressure and have higher faradaic efficiencies.

2.3 Effect of pressure on selectivities

Electrostriction-driven selectivities. The main rule governing the kinetics under compression is Le Chatelier's principle, which follows from the thermodynamic relation (eqn (4)) that the change in free energy with pressure at constant temperature equals the standard reaction volume. Hence, a process that involves a net decrease in volume is favored by an increase in pressure. When charged species interact strongly with a polar solvent, it causes a macroscopic compressive effect called electrostriction, which can be so pronounced for highly solvated species that it leads to negative partial molar volumes of reaction. For instance, the dissociation of an electrolyte in an aqueous solution. Here, due to electrostriction, the arrangement of the solvent molecules around the products (ions) is more compact than around the reactants (neutral species), causing a net decrease in reaction volume. Therefore, the dissociation process is promoted with increasing pressure. Han *et al.*[45] describe a method to do electrochemical impedance spectroscopy at high pressures in a diamond anvil cell to study the electrostrictive properties of materials.

A similar electrostriction effect is also applicable to redox reactions. Electrostriction makes the arrangement of solvent molecules more compact around the products than the reactants, which promotes the redox reaction.[44] For example, the conversion of N_2 (neutral species) to NO_3^- or NH_4^+ (charged species) will be promoted due to electrostriction, whereas the competing reactions (OER: OH^- to O_2, or HER: H^+ to H_2) involving the formation of neutral (less polar) species will be suppressed due to positive volume of reaction.

The volume change due to electrostriction is driven by higher local electrostatic interaction between the solute and solvent, which is counterbalanced by the internal pressure of the solvated ion at equilibrium. This equilibrium is described by the following model,[46]

$$\frac{1}{V}\left(\frac{\partial V}{\partial E}\right)_{\mu,T} = -\left(\frac{E}{4\pi}\right)\left(\frac{\partial \varepsilon}{\partial P}\right)_{E,T} \quad (6)$$

where V is the volume of the electrolyte, E is the local electric field between solute and solvent, μ is the chemical potential, ε is the dielectric constant, and T is the temperature. The above equation can be solved to obtain the volume change due to electrostriction, which could be substituted in eqn (5) to obtain a reduction in equilibrium potential and thereby thermodynamic selectivity of competing redox reactions. A numerical estimate for the effect of pressure on the volume change due to electrostriction for the ferrocene/ferrocenium system in 1 M $NaClO_4$ is provided by Faulkner *et al.*[47]

Effect of pressure on corrosion. At higher pressures, the corrosion can sometimes be accelerated, as in deep ocean conditions. It has been reported by Yang *et al.*[48] and Sun *et al.*[49] that the steel could be corroded due to the influence of hydrostatic pressure and seawater erosion. It has also been reported that the corrosion rate will increase with increased pressure of an oxidant.[50] Having said that, the corrosion stability can be improved at high pressures in specific electrochemical systems.

High pressures could suppress the formation of corrosive gases such as O_2, thereby mitigating their detrimental effects on the electrode materials. Certain electrolytes that offer corrosion protection by acting as inhibitors or passivating agents will exhibit improved solubility, thereby providing better protection to the electrode surfaces and reducing the corrosion rate. An increase in the pressure will increase the redox potential of the metal oxidation.[51] The corrosion lines in the Pourbaix diagram will shift up (by 1%) with increasing pressure (by 200 bar) and stabilize the electrocatalysts under oxidation conditions. Hence, we hypothesize that the catalysts for CH_4 oxidation to CH_3OH will be stable at elevated pressures, which is a common challenge. High-pressure studies can be explored for other studies, such as water electrolysis in an acidic medium where catalyst stability is a significant challenge.

2.4 Effect of pressure on the electrode–electrolyte interface

Higher capacitance of the electric double layer at elevated pressure. The composition and structure of the EDL vary with increasing pressures, and this affects the reactivity at the electrochemical interfaces. Although there is a minimal set of experimental studies on the dynamics of the EDL at high pressures, the conceptual framework of the Poisson–Boltzmann equation can provide a pressure-dependent response of electric potential in the EDL. The compression of the electrolyte increases the dielectric constant and reduces the exclusion volume.[52] The combined effect of higher dielectric constant and lower exclusion volume causes the capacitance of the EDL to increase with an increase in pressure. This is also associated with the increased charge density and the local electric field in the Helmholtz plane. The pressure-enhanced local electrical field will stabilize the reaction intermediates of desired reactions, possibly leading to higher selectivities. The structural change in the EDL can be understood from the electrochemical impedance spectroscopy (EIS) at high pressures. Fig. 6 represents a schematic of the EDL at extreme pressures.

Pressure-potential (surface) pourbaix diagram. In addition to the electrolyte phase of the double layer, pressure as an independent variable can have a significant effect on the expected coverage of reactants on a surface. As an example, below we explore the implications of elevated N_2 pressure on the non-Li mediated N_2 reduction reaction (N_2RR). Fig. 7A illustrates the predicted coverage of N_2 (θ_{N_2}) on BCC Fe (100) and W (100). Several simplifications were made in the construction of these phase diagrams. The coverages presented in Fig. 7B represent Boltzmann representations of three states: hydrogen coverage (θ_H) resulting from *e.g.*, the Volmer reaction, dinitrogen coverage, and an empty site (θ_*), with the relative coverage of dinitrogen given by the equation,

$$\theta_{N_2} = \frac{e^{-\frac{\Delta G_{N_2}}{k_B T}}}{1 + e^{-\frac{\Delta G_{N_2}}{k_B T}} + e^{-\frac{\Delta G_H}{k_B T}}} \quad (7)$$

As before, binding energies of N_2 and H_2 were calculated using semi-local DFT. Entropic contributions in the adsorbed
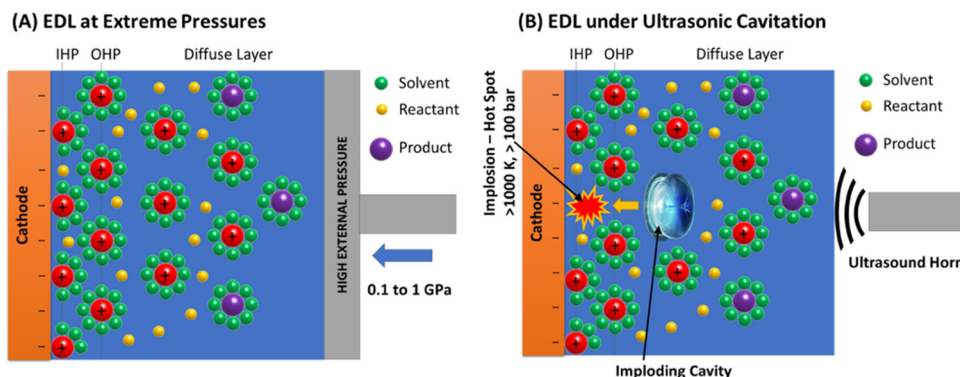
Fig. 6 Schematic of the electrical double layer (EDL) at extreme pressures induced by either a positive overhead pressure or ultrasound.

state were assumed to be entirely vibrational and approximated as a harmonic oscillator. The gas phase state was approximated as an ideal gas, which may not hold above e.g., 10^6 bar at room temperature. By construction, the coverages are normalized such that $1 = \theta_{N_2} + \theta_H + \theta_*$. An interesting observation is seen in Fig. 7A, where we find a pressure of $\sim 10^{3-4}$ bar is needed for N_2 to appreciably adsorb on Fe (100) at the RHE equilibrium potential. There are several important deviations from our model catalyst system (clean Fe (100)) and e.g., the industrial Haber–Bosch catalyst, which operates at pressures of 100–150 bar. It has long been known that the rate-determining step, i.e., N_2 activation, takes place on the steps of catalysts[53] (whether Ru or Fe), and in the presence of one of several alkali metal

promoters.[54] Furthermore, the industrial reaction occurs at high temperature, which would improve the needed pressure for appreciable N_2 coverage in Fig. 7A. A more complete picture would be given by a complete N_2RR microkinetic model. Such a model would incorporate much stronger binding states, e.g., *N, which may dominate the coverage of an actual Haber–Bosch catalyst.

In general, competition between N_2 and H adsorption can be understood by the scaling shown in Fig. 8. Here, we see a poor scaling between these two states, though nearly all of the tested transition metals favor H adsorption over dinitrogen. An ideal catalyst candidate for the N_2RR process will bind N_2 more strongly than H, but without binding ammonia so strongly that the catalyst becomes poisoned by products. If the slope of the (black dashed) scaling line holds, then perhaps weak binding catalysts (i.e., with high d band centers[55]) will favor N_2 binding over H at lower pressures. Naturally, weak binding catalysts like Cu will struggle to dissociate N_2 at room temperature, but if a strong reducing bias can be applied without compromising N_2 coverage, such a reaction may not be necessary like in the thermochemical process. Instead, dissociation of *N_2H or *N_2H_2 may be more facile. Alternatively, weak binding catalysts doped with single atoms of a strong binding catalyst may be a promising system for future investigation.

2.5 Effect of pressure on the electrolyte conductivity

Higher viscosity and lower mobility at higher pressures. The viscosity of the electrolyte, in most cases, increases with
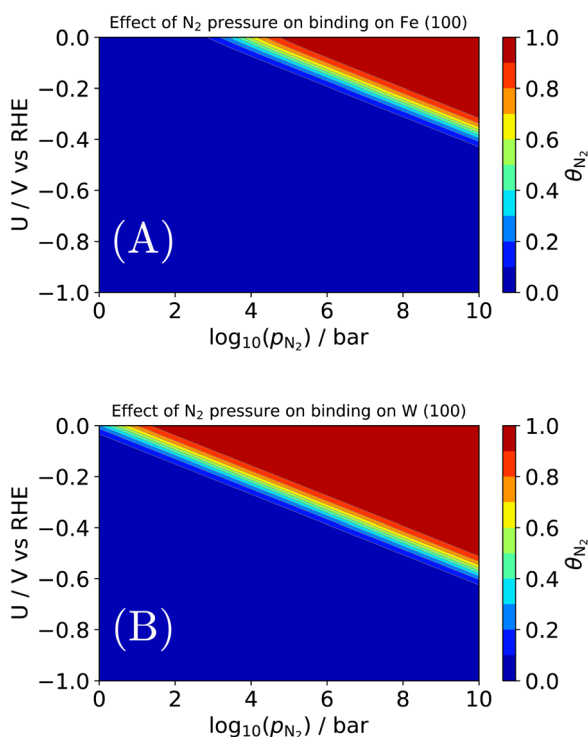

Fig. 7 Effect of N_2 pressure on the equilibrium coverage of *N_2 on two candidates for an electrochemical Haber–Bosch process: (A) the terrace of Fe (100); (B) the terrace of W (100).
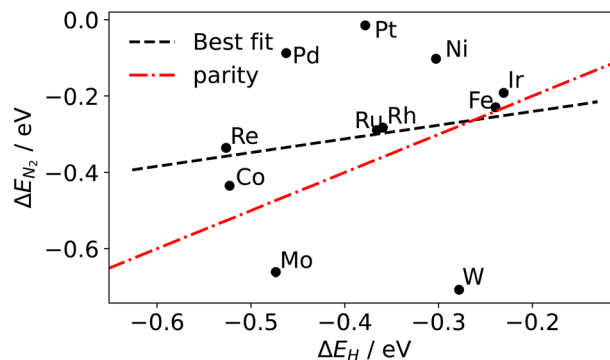

Fig. 8 Scaling of dinitrogen binding with hydrogen binding energetics.

increasing pressure. The exemption to this behavior is observed at temperatures $< 10\ ^{\circ}$C and concentrations < 0.1 M.[56,57] The increase in viscosity of the solvent also impedes the mobility of ions according to the Stokes–Einstein equation. The lower mobility results in lower ionic conductivity and higher ohmic losses. The effect of pressure on viscosity is generally given by an empirical equation known as the Barus equation,[58] denoted by,

$$\eta_P = \eta_0 \exp(\alpha P) \tag{8}$$

where η_P denotes the viscosity at pressure P, η_0 denotes the viscosity at ambient pressure, and α denotes the pressure viscosity coefficient $(\mathrm{m}^2\ \mathrm{N}^{-1})$. As we can see from the equation, the viscosity increases exponentially as a function of the pressure.

Higher activity coefficient at elevated pressures. The effect of pressure on the activity coefficient is determined from the relationship that the derivative of chemical potential with respect to pressure is equal to the partial molar volume.[59]

$$\left(\frac{\partial \ln \gamma_{\pm}}{\partial P}\right)_T = \frac{\bar{V}}{\upsilon RT} \tag{9}$$

where $\gamma_{\pm}$ denotes the mean molar activity coefficient of an electrolyte, $\bar{V}$ denotes the partial molar volume and υ denotes the no. of moles of ions into which a mole of electrolyte dissociates. For 1–1 electrolyte (*e.g.*, HCl and HNO_3) of molar volume 30 $\mathrm{cm}^3\ \mathrm{mol}^{-1}$ at 25 $^{\circ}$C, the change in activity coefficient with pressure is $\sim 6 \times 10^{-4}\ \mathrm{bar}^{-1}$. This suggests that the activity coefficient increases by $\sim 6\%$ with an increase in pressure to 100 bar. The increase in activity coefficient will increase the conductivity of the electrolyte by increasing the concentration of free ions in the solution.

3. Experimental tools for high-pressure electrochemistry

In contrast to ambient-pressure electrochemical studies, high-pressure electrochemical studies require a new frontier in instrumentation defined by innovative tools that allow observation, understanding, and control of complex, dynamic, and hierarchical catalytic processes. Performing electrochemical experiments at elevated pressures (>200 bar) is challenging, and reactors/instruments must be designed for safe operation. Realizing extreme conditions in the confines of a laboratory setting is a formidable challenge, especially characteristics that include extreme pressures coupled with corrosive or contaminating fluids and gases, high electric fields, and highly heterogeneous sample environments. The development of capabilities to evaluate processes under extreme conditions is needed across the disciplines of materials and chemistry. To study high-pressure electrochemistry, progress is required to develop novel electrochemical reactors operating at extreme pressures. For example, we do not have (i) high-pressure electrochemical reactors and their stacks that can withstand >200 bar, (ii) high-throughput screening tools for electrochemical synthesis at high pressures, and (iii) high-pressure electrochemical cells for operando FTIR, Raman, NMR, XAS, ambient XPS, and neutron scattering experiments.

A range of high-pressure electrochemical reactors with different capacities and capabilities are available (see Fig. 9). These are – (i) high-pressure (<0.04 GPa/400 bar) batch and continuous reactors of 10 to 1000 mL volumes with better gas management, (ii) very high pressure (1–10 GPa) Paris–Edinburgh reactors of 0.1–1 mL volume, and (iii) ultrahigh pressure (10–100 GPa) Diamond Anvil Cell (DAC) reactors with < 0.1 nL volumes.

As shown in Fig. 9, various apparatuses are available to push the capabilities of electrochemistry to very high pressure, above 1 GPa, such as the cubic anvil press,[60] Paris–Edinburgh (PE) cell,[61] and the piston-cylinder.[62–64] Such apparatus is used to study the electrochemical properties at elevated pressures for systems involving extreme pressures, such as oceanographic, geothermal, and exoplanet explorative studies. Systematic adaptation of these apparatuses to an electrochemical cell stack and simultaneous characterization probes that can be used to conduct the electrochemical synthesis of chemicals at elevated pressures is required. The high-pressure electrochemical cells must be configured to place electrodes connected to a potentiostat to control potentials.
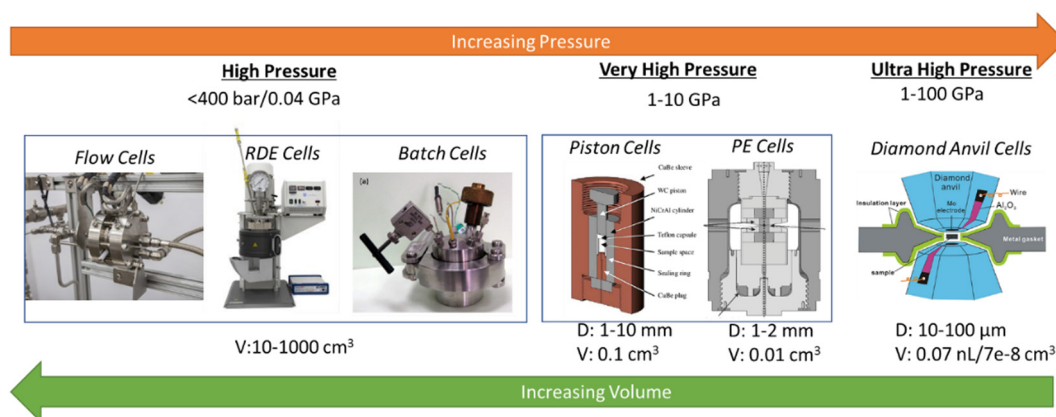

Fig. 9 Range of high-pressure electrochemical reactors with varying volume and pressure levels.
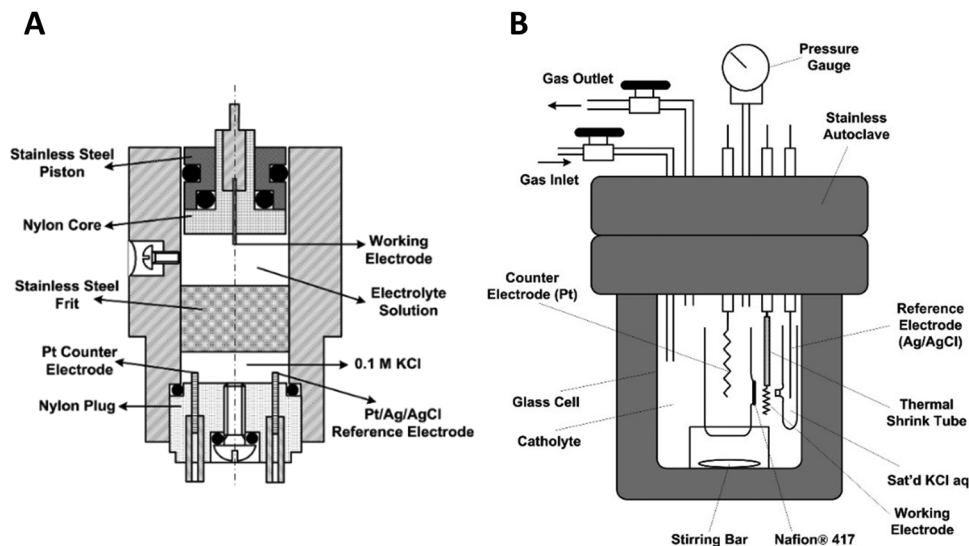
Fig. 10 Schematic of a modified autoclave to place the electrodes for high-pressure electrochemical synthesis (adapted from (Cruanes et al.,[44]; and (Hara et al.,[33] 1995)). Copyright 1992 American Chemical Society, and Copyright 1995 Elsevier B.V. The electrochemical cell is placed inside the autoclave and the gas is pressurized using a compressor.

Fig. 10A shows a detailed schematic of the piston-based high-pressure cell, and Fig. 10B shows a schematic of the modified autoclave to perform high-pressure electrochemical synthesis. The schematic of these designs is taken from Cruanes et al.,[44] and Hara et al.[33] Autoclaves usually are designed to carry out reactions at high temperatures and pressures. The existing autoclaves must be modified to insert three electrodes to carry out the electrochemical reactions. Autoclaves are generally made of stainless steel; hence, they cannot be used directly to perform electrochemical reactions. Either the walls of the autoclave have to be coated with an insulating material like Teflon, or a separate electrochemical cell made of glass or polypropylene has to be placed inside the autoclave. The electrochemical cell has to be designed based on the autoclave dimensions. The other approach to pressurizing is by using a piston, which is commonly employed to pressurize liquid-based systems.

Increased pressure *in situ*/operando electrochemical arrangements for Fourier transform IR (FTIR) spectroscopy, X-ray absorption spectroscopy (XAS), ambient pressure X-ray photoelectron spectroscopy (AP-XPS), and nuclear magnetic resonance (NMR) spectroscopy are not currently available. AZO materials sell a high-pressure, high-temperature FTIR cell to analyze solid samples (denoted by Fig. S3A, ESI†), which can be modified to perform operando electrochemical reactions at high pressures. A setup used in (a) FTIR and (b) UV-Vis determinations showing the high-pressure view cell coupled to the respective spectrophotometers is shown in Fig. 11a and b, respectively. A schematic of the custom-built *operando* Raman system with the high-pressure H-cell is shown in Fig. 11c. A flat and beveled diamond anvil for generating high pressures is shown in Fig. 11d. In addition, a range of diamond anvil cells (DACs) are sold by Almax easyLab Inc. (Fig. S3B, ESI†) which can be used for testing the properties of materials using

electrochemical impedance spectroscopy as described by Han et al.[65] The method can be modified and extended for other fundamental electrochemical studies. Fig. 11e represents an assembled rotational tomographic Paris Edinburgh cell device, which is a portable press for micro-tomographic 4-D imaging at extreme pressure conditions and Paris-Edinburgh cells developed at Oakridge National Laboratory (Fig. S3C, ESI†) are used for neutron diffraction studies, and such cells can be modified for *in situ* XAS and operando ambient pressure XPS studies at high pressures. Parr Instrument Company sells several modified autoclave designs for high-pressure electrochemical synthesis. Fig. S4 (ESI†) show a few of the commercially available high-pressure reactors, including a high-pressure batch electrochemical cell, a high-pressure rotating disc electrode (RDE) setup, and a high-pressure continuous electrochemical cell. Commercial autoclave setups available for high-pressure electrochemical studies like electrochemical reduction of CO_2 to formic acid/formate and electrochemical synthesis of ammonia are shown in Fig. 12.

4. Operation of high-pressure electrochemical reactors

Differential pressure operation

Differential pressure operation involves maintaining different pressures in the anode and the cathode chambers of the electrolyzers. Differential pressure operation has numerous advantages as well as disadvantages. One of the significant advantages of differential pressure operation is the reduction in product crossover, especially at low current densities. By maintaining a higher pressure at the anode than the cathode, the migration of products from the anode to the cathode will be mitigated, resulting in improved selectivity and purity of the
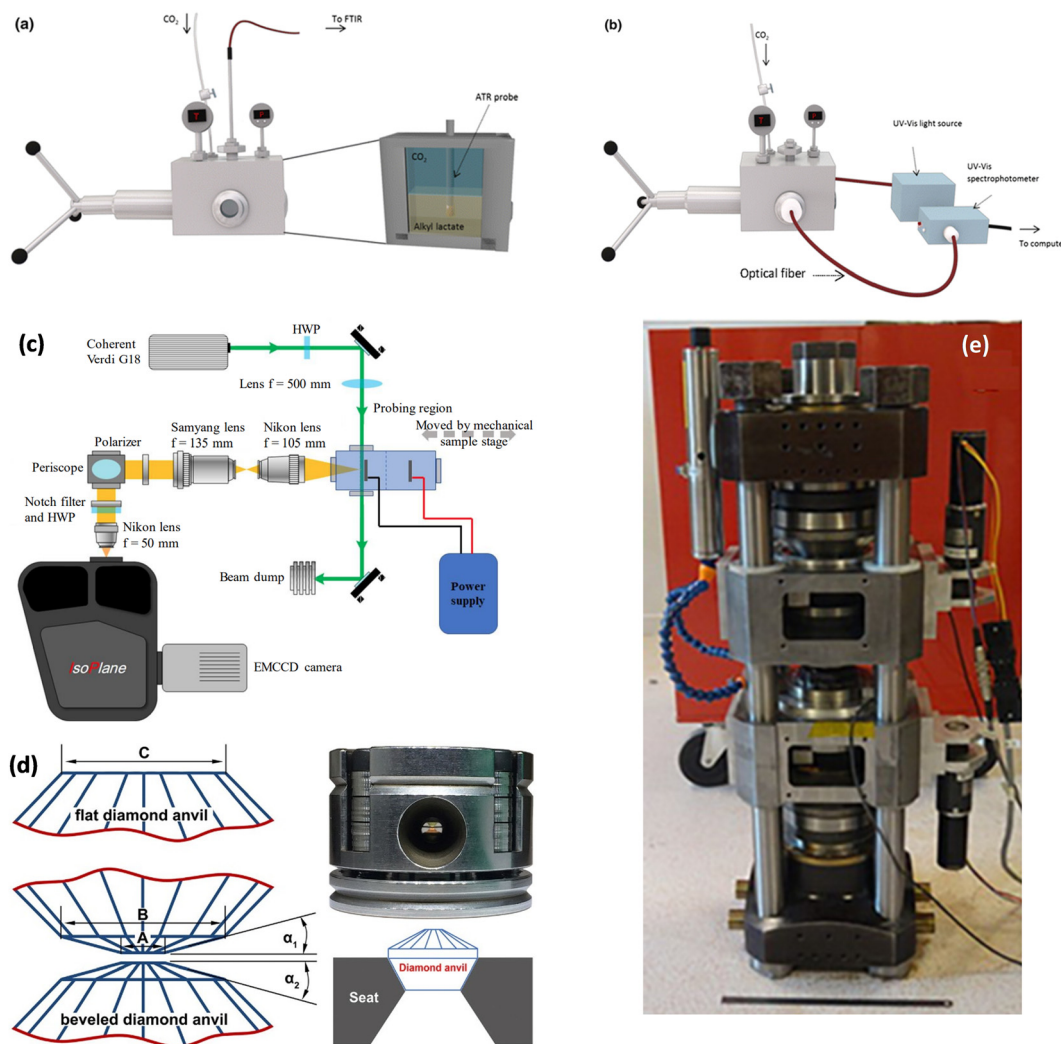
Fig. 11 Instrumentation for fundamental electrochemical studies at higher pressures: setup used in (a) FTIR and (b) UV-Vis determinations showing the high-pressure view cell coupled to the respective spectrophotometers, Adapted from Medina-Gonzalez et al.[66] Copyright 2017 Springer Science Business Media New York. (c) Schematic of the custom-built operando Raman system with the high-pressure H-cell, Adapted from Ramdin et al.[35] Copyright 2019 American Chemical Society. (d) Flat and beveled diamond anvils for generating high pressures, Adapted from Li et al.[67] Copyright 2018 Published under the PNAS license. (e) Assembled rotational tomographic Paris Edinburgh cell device which is a portable press for micro-tomographic 4-D imaging at extreme pressure conditions, Adapted from Philippe et al.[68] Copyright 2016 The Author(s). Published by Informa UK Limited, trading as Taylor & Francis Group.

product gases. Differential pressure operation can help retain the electrolyte within the cell by reducing the risk of electrolyte loss due to evaporation or other factors. This helps improve the selectivity of the gas evolution reactions, leading to improved control over the desired product generation. One of the disadvantages of differential pressure operation is the complicated system design and the requirement of additional pressure control mechanisms and safety measures needed to maintain pressure differentials. Differential pressure operation has a risk of H_2 crossover, where H_2 can permeate through the membrane and impact the cell efficiency and product purity. Differential pressure operation could lead to variation in the electrolyte concentration between the compartments, affecting the reaction rates and the overall system performance. Pressurization of both compartments ensures uniform conditions and

simplifies the system design. However, differential pressure operation has unique advantages, as mentioned above.

Dynamic operation

Dynamic operation of an electrochemical system refers to dynamically changing the operating conditions based on the price and availability of renewable energy sources. Pressurization affects the dynamic operation of electrochemical processes such as PEM electrolyzers. Pressurization affects the response time and efficiency during dynamic operation. The system requires more controls for rapidly shifting between high and low operating current densities. Pressurization can improve electrode stability by minimizing the concentration polarization and electrode kinetics and could maintain consistent H_2 production rates during fluctuating energy inputs. The relationship
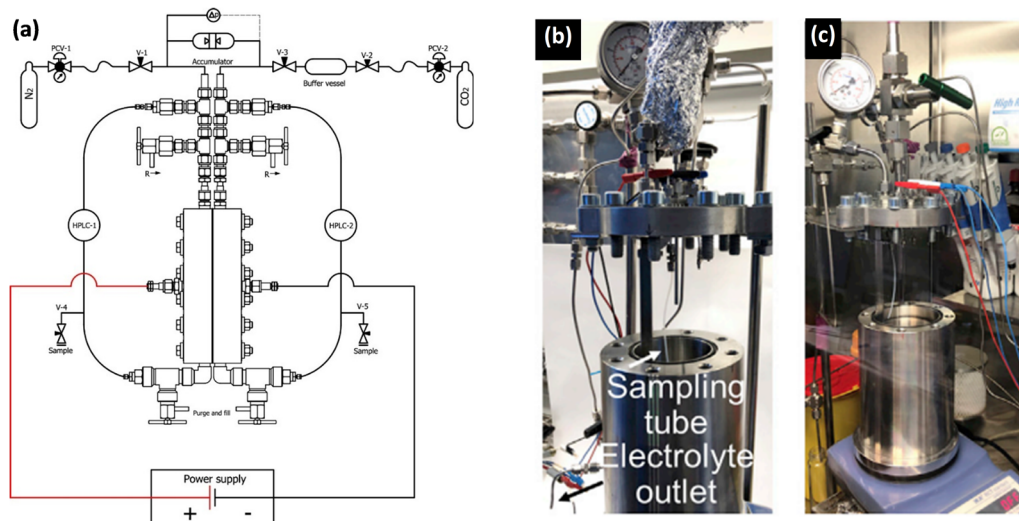
Fig. 12 Examples of autoclave setups developed for high-pressure electrochemical studies. (a) A schematic of a continuous-flow high-pressure setup for electrochemical reduction reaction,[1] Adapted from Ramdin *et al.*[35] Copyright 2019 American Chemical Society. Photos of batch autoclave reactors placed in (b) the fume hood and (c) the Ar glovebox for electrochemical synthesis of ammonia. Adapted from Li *et al.*[69] Copyright 2022 The Author(s). Published by Elsevier Inc.

between pressure, current densities, and the cost of renewable electricity must be carefully analyzed to get a pressure range that offers the best efficiency during the dynamic operation. It can impact heat generation and dissipation within the electrochemical system, and efficient heat management systems are important for stable operation and preventing overheating during dynamic load changes. Pressurization has several advantages for operating the systems dynamically but requires better system control and heat management techniques.

Safety precautions for operating high-pressure electrochemical systems

Safety requirements are essential when dealing with high-pressure electrochemical systems. A comprehensive discussion of the safety measures is provided in this section to ensure that early-stage researchers who might be less experienced understand the potential hazards and carry out the experiments safely and responsibly.

Material compatibility and efficient design: It needs to be ensured that the reactors are built using materials that can withstand operating conditions and resist corrosion from the reactants and products. All reactor vessels, fittings, sealants, and other components need to be designed and constructed to withstand beyond the operating pressure to ensure safe operation. Refer to ASTM standards while designing reactors and other components like sealants and fittings to withstand high pressures. And always operate a high-pressure reactor in a blast-proof chamber.

Pressure relief devices: Fail-safe mechanisms such as rupture discs and pressure relief valves must be installed to prevent over-pressurization. Over-pressure protection systems need to be set to release at a pressure slightly above the operating pressure of the reactor. The pressure relief systems must be

routinely tested and maintained to ensure proper functioning. Refer to ASTM standards for adequate choice for fail-safe mechanisms.

Documentations: A detailed standard operating procedure (SOP) must be developed to operate the high-pressure electrochemical reactors. A detailed record of all the experiments performed, safety checks, maintenance checks, operating conditions, and any deviations from the SOP must be maintained.

Operator training: Comprehensive training must be provided to all personnel operating the high-pressure electrochemical reactor to follow the SOP. It needs to ensure that the operators understand the principles of electrochemistry, pressurization, and the potential hazards associated with the processes.

Emergency response plan: A detailed emergency response plan should be in place that outlines the steps to be followed in case of leaks, fires, and explosions. Regular drills and training exercises must be conducted to ensure all personnel are familiar with the emergency response procedures.

Regular maintenance and inspection: A regular maintenance schedule for high-pressure electrochemical reactors and associated instruments must be conducted. Also, regular inspections, calibration of the pressure sensors, and replacement of damaged or worn-out components need to be performed.

It is essential to involve safety engineers, design experts, and other authorities to ensure that the design, operation, and maintenance of high-pressure electrochemical reactors are performed at the highest level of safety for the operating personnel and the environment.

5. Economic considerations

The primary motivation for high-pressure electrochemistry is to realize higher current density and reduce the energy

consumption (or cell voltage) of the process. Fig. 2 shows that there could be a net reduction in electrical energy requirement to operate an electrochemical reactor at high pressure compared to ambient pressures. However, the high-pressure operation requires thick-walled reactors, which are more expensive than ambient-pressure reactors.

The higher operating current density at high pressure also helps in reducing the number of reactors and, thereby, capital cost. For example, consider an electrochemical reaction operating at 1 mA cm^{-2} at 1 atm that is scaled up using 100 electrochemical cells of 10 cm^2 area each to attain a total operating current of 1 A for 100 cells. Since the current density varies linearly with the pressure of reactants, increasing the pressure to 100 atm is expected to increase the current density to 100 mA cm^{-2}. Now, scaling up the 100 atm reactors to attain an overall current of 1 A will require 1 electrochemical cell of 10 cm^2 area. This linear dependence of current density on the pressure results in two capital (or reactor) choices – the first choice is 100 cells operating at 1 atm and the second choice is 1 cell operating at 100 atm. Choosing a high-pressure reactor can result in a significant reduction in footprint and some savings in capital investment.

Fig. 13 shows the estimated cost of mild steel as a function of the size of the reactor that can withstand up to 100 bar (adapted from the book on Chemical Engineering Economics by Garrett).[70] It can be observed that the cost of the material and the reactor increases exponentially as the size of the reactor increases. For decentralized production, the volume of the reactor will be less than 100 gallon and the estimated cost of the material is much less. We note that the original estimate made in the book is based on the 1989 data and inflation has to be taken into account, but the order of reduction in cost would be the same as the ones reported.
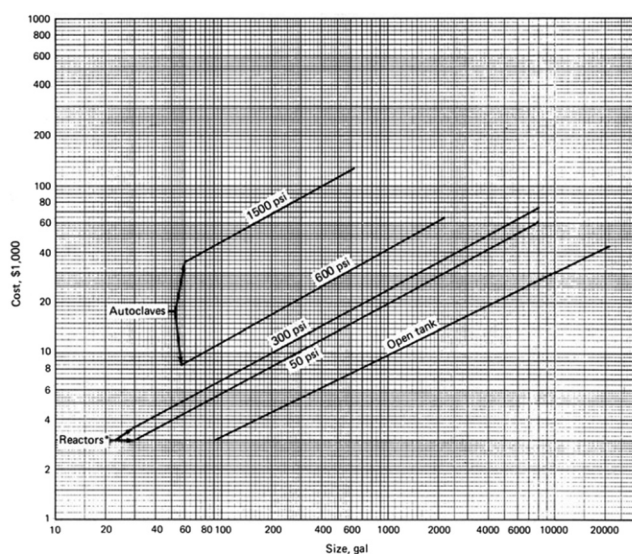

Fig. 13 Cost of mild steel as a function of the size of the reactor and operation pressures. Figure adapted from Chemical Engineering Economics by Garrett.[70]

6. Challenges of high-pressure electrochemistry

High-pressure electrochemistry requires specialized and often complex equipment, including pressure vessels, seals, and safety measures. These components can be costly to acquire, maintain, and operate. Additionally, the complexity of the system may introduce additional sources of experimental variability and potential points of failure. High-pressure experiments entail inherent safety risks. The presence of pressurized gases or liquids increases the potential for leaks, ruptures, or explosions, posing risks to researchers and the laboratory environment. Proper safety protocols, training, and infrastructure are crucial to mitigate these hazards effectively. A detailed safety precautions procedure is provided in Section 4. Not all electrochemical cells, electrodes, or catalyst materials may be compatible with high-pressure conditions. The corrosive nature of certain electrolytes or the instability of electrode materials at high pressures can limit the range of materials that can be used in high-pressure electrochemistry experiments. Elevated pressures can significantly affect the transport of reactants and products within the electrochemical cell. Increased viscosity and reduced diffusion coefficients can impede mass transport, leading to slower reaction rates and limiting the overall performance of the system. High-pressure electrochemical reactions may involve intricate kinetic pathways and complex reaction mechanisms. Understanding and modeling these reactions can be challenging, requiring advanced theoretical approaches and computational resources. Conducting experiments at high pressures introduces technical challenges. Ensuring uniform pressure distribution, preventing leaks, and accurately measuring and controlling reaction parameters are complex tasks that require specialized expertise. These challenges can impact data quality and reliability. Scaling up high-pressure electrochemical processes for practical applications can be challenging. Designing and constructing large-scale high-pressure systems, along with ensuring safety and reliability, pose significant engineering and operational hurdles that need to be addressed. Gas crossover is one of the key challenges associated with pressurization. Gas crossover refers to the unintended transfer of gases across the membranes in electrochemical systems. This could be predominant if one of the cathode/anode sides is pressurized. This would lead to reduced efficiency (due to undesired side reactions) and higher energy consumption, and affect the purity of the product gases. Potential safety concerns can arise if the gas crossing could lead to mixing reactive gases on the opposite sides of the cell. The gas crossover can be prevented by choosing an appropriate membrane material with low gas permeability or *via* further processing, such as annealing.[71]

7. Conclusions and outlook

High-pressure electrochemical synthesis of chemicals is in the nascent stages of development. The prospect of using elevated

pressures is to overcome the existing challenges in the electrochemical synthesis of chemicals that involve gas phase reactants, which tend to have lower activities and selectivities. High pressures require lesser energy compared to high-temperature operation; hence, high-pressure electrochemical synthesis of chemicals can be scaled up for the decentralized production of chemicals, and the capital cost will be considerably less for the decentralized production as the volume of the reactor is an exponential function of the cost. The theory behind the improvement in the electrochemical reaction performance, including activity, selectivity, stability, and energy efficiency at elevated pressures, is discussed. For high-pressure electrochemistry – (i) the energy requirement is lower due to the Nernst effect and selective absorption of gases, (ii) the current densities are higher due to higher solubility, lower overpotential, and high exchange current density, (iii) the selectivities can be better due to electrostriction, a higher separation between reduction lines or oxidation lines in the Pourbaix diagram, higher stabilization of intermediates, and higher surface coverages of reactants, and (iv) improved stability due to the increase in the oxidation potential of the catalyst. The electrical conductivity does decrease with increasing pressure, which could result in higher ohmic losses.

We emphasize the need for novel high-pressure reactors for the synthesis of chemicals and operando tools for understanding the reaction mechanisms. High-pressure electrochemical synthesis could be a paradigm shift in the decarbonization of chemical manufacturing, and the justifications provided in this work would motivate researchers to explore the field.

Conflicts of interest

There are no conflicts to declare.

Acknowledgements

References

1 R. Sharifian, R. Wagterveld, I. Digdaya, C. Xiang and D. Vermaas, *Energy Environ. Sci.*, 2021, **14**, 781–814.

2 M. Fajardy, A. Köberle and N. Macdowell, BECCS deployment: a reality check. Report for the Grantham Institute, Imperial College London, Report, 2018.

3 D. S. Mallapragada, Y. Dvorkin, M. A. Modestino, D. V. Esposito, W. A. Smith, B.-M. Hodge, M. P. Harold, V. M. Donnelly, A. Nuz and C. Bloomquist, *Joule*, 2023, **7**, 23–41.

4 Z. J. Schiffer and K. Manthiram, *Joule*, 2017, **1**, 10–14.

5 N. C. Kani, A. Prajapati, B. A. Collins, J. D. Goodpaster and M. R. Singh, *ACS Catal.*, 2020, **10**, 14592–14603.

6 A. R. Singh, B. A. Rohr, J. A. Schwalbe, M. Cargnello, K. Chan, T. F. Jaramillo, I. Chorkendorff and J. K. Nørskov, *ACS Catal.*, 2017, DOI: **10.1021/acscatal.6b03035**.

7 M. A. Shipman and M. D. Symes, *Catal. Today*, 2017, **286**, 57–68.

8 N. Lazouski, M. Chung, K. Williams, M. L. Gala and K. Manthiram, *Nat. Catal.*, 2020, **3**, 463–469.

9 K. Li, S. Z. Andersen, M. J. Statt, M. Saccoccio, V. J. Bukas, K. Krempl, R. Sažinas, J. B. Pedersen, V. Shadravan and Y. Zhou, *Science*, 2021, **374**, 1593–1597.

10 H.-L. Du, M. Chatti, R. Y. Hodgetts, P. V. Cherepanov, C. K. Nguyen, K. Matuszek, D. R. MacFarlane and A. N. Simonov, *Nature*, 2022, **609**, 722–727.

11 J. Choi, H.-L. Du, C. K. Nguyen, B. H. Suryanto, A. N. Simonov and D. R. MacFarlane, *ACS Energy Lett.*, 2020, **5**, 2095–2097.

12 S. Z. Andersen, V. Čolić, S. Yang, J. A. Schwalbe, A. C. Nielander, J. M. McEnaney, K. Enemark-Rasmussen, J. G. Baker, A. R. Singh and B. A. Rohr, *Nature*, 2019, **570**, 504–508.

13 N. C. Kani, A. Prajapati and M. R. Singh, *ACS ES&T Engg.*, 2022, **2**(6), DOI: **10.1021/acsestengg.1c00484**.

14 N. C. Kani, J. A. Gauthier, A. Prajapati, J. Edgington, I. Bordawekar, W. Shields, M. Shields, L. C. Seitz, A. R. Singh and M. R. Singh, *Energy Environ. Sci.*, 2021, **14**(12), DOI: **10.1039/D1EE01879E**.

15 N. C. Kani, N. H. L. Nguyen, K. Markel, R. R. Bhawnani, B. Shindel, K. Sharma, S. Kim, V. P. Dravid, V. Berry, J. A. Gauthier and M. R. Singh, *Adv. Energy Mater.*, 2023, **13**(17), DOI: **10.1002/aenm.202204236**.

16 W. Liu, P. Zhai, A. Li, B. Wei, K. Si, Y. Wei, X. Wang, G. Zhu, Q. Chen and X. Gu, *Nat. Commun.*, 2022, **13**, 1877.

17 H. S. Jeon, S. Kunze, F. Scholten and B. Roldan Cuenya, *ACS Catal.*, 2018, **8**, 531–535.

18 A. Prajapati, N. C. Kani, J. A. Gauthier, R. Sartape, J. Xie, I. Bessa, M. T. Galante, S. L. Leung, M. H. Andrade and R. T. Somich, *Cell Rep. Phys. Sci.*, 2022, **3**, 101053.

19 D. Yang, Q. Zhu, C. Chen, H. Liu, Z. Liu, Z. Zhao, X. Zhang, S. Liu and B. Han, *Nat. Commun.*, 2019, **10**, 677.

20 A. H. B. Mostaghimi, T. A. Al-Attas, M. G. Kibria and S. Siahrostami, *J. Mater. Chem. A*, 2020, **8**, 15575–15590.

21 A. Prajapati, R. Sartape, N. C. Kani, J. A. Gauthier and M. R. Singh, *ACS Catal.*, 2022, **12**, 14321–14329.

22 L. Adams, *J. Am. Chem. Soc.*, 1931, **53**, 3769–3813.

23 L. Adams and R. Hall, *J. Washington Acad. Sci.*, 1931, **21**, 183–194.

24 L. Adams and R. Hall, *J. Phys. Chem.*, 2002, **35**, 2145–2163.

25 E. Cohen, *ZS. Physik. Chem. (A)*, 1934, **167**, 365.

26 D. Giovanelli, N. S. Lawrence and R. G. Compton, *Electroanalysis*, 2004, **16**, 789–810.

27 G. Schneider, *Berichte der Bunsengesellschaft für physikalische Chemie*, 1972, **76**, 325–331.

28 G. Hills and D. Kinnibrugh, *J. Electrochem. Soc.*, 1966, **113**, 1111.

29 A. Gancy and S. Brummer, *J. Electrochem. Soc.*, 1968, **115**, 804.

30 A. Ewald and S. Lim, *J. Phys. Chem.*, 1957, **61**, 1443–1445.

31 M. B. Towns, R. S. Greeley and M. Lietzke, *J. Phys. Chem.*, 1960, **64**, 1861–1863.

32 P.-W. Guan, R. J. Hemley and V. Viswanathan, *Proc. Natl. Acad. Sci. U. S. A.*, 2021, **118**, e2110470118.

33 K. Hara, A. Kudo and T. Sakata, *J. Electroanal. Chem.*, 1995, **391**, 141–147.

34 M. Todoroki, K. Hara, A. Kudo and T. Sakata, *J. Electroanal. Chem.*, 1995, **394**, 199–203.

35 M. Ramdin, A. R. Morrison, M. De Groen, R. Van Haperen, R. De Kler, L. J. Van Den Broeke, J. M. Trusler, W. De Jong and T. J. Vlugt, *Ind. Eng. Chem. Res.*, 2019, **58**, 1834–1847.

36 L. M. Welch, M. Vijayaraghavan, F. Greenwell, J. Satherley and A. J. Cowan, *Faraday Discuss.*, 2021, **230**, 331–343.

37 J. Lee, J. Yang and J. H. Moon, *ACS Energy Lett.*, 2021, **6**, 893–899.

38 R. S. Kim and Y. Surendranath, *ACS Cent. Sci.*, 2019, **5**, 1179–1186.

39 E. M. Lee, T. Ludwig, B. Yu, A. R. Singh, F. Gygi, J. K. Nørskov and J. J. de Pablo, *J. Phys. Chem. Lett.*, 2021, **12**, 2954–2962.

40 M. Jørgensen and H. Gronbeck, *J. Phys. Chem. C*, 2017, **121**, 7199–7207.

41 A. Bajpai, P. Mehta, K. Frey, A. M. Lehmer and W. F. Schneider, *ACS Catal.*, 2018, **8**, 1945–1954.

42 P. K. Frolich, E. Tauch, J. Hogan and A. Peer, *Ind. Eng. Chem.*, 1931, **23**, 548–550.

43 R. Nakhaei-Kohani, E. Taslimi-Renani, F. Hadavimoghaddam, M.-R. Mohammadi and A. Hemmati-Sarapardeh, *Sci. Rep.*, 2022, **12**, 3625.

44 M. T. Cruanes, H. G. Drickamer and L. R. Faulkner, *J. Phys. Chem.*, 1992, **96**, 9888–9892.

45 T. Han, H. Liu, J. Wang, C. Gao and Y. Han, *J. Phys. Chem. C*, 2021, **125**, 8788–8793.

46 J. Desnoyers, R. Verrall and B. Conway, *J. Chem. Phys.*, 1965, **43**, 243–250.

47 M. T. Cruanes, H. G. Drickamer and L. R. Faulkner, *Langmuir*, 1995, **11**, 4089–4097.

48 Z. Yang, B. Kan, J. Li, Y. Su and L. Qiao, *Int. J. Hydrogen Energy*, 2017, **42**, 27446–27457.

49 F. Sun, S. Ren, Z. Li, Z. Liu, X. Li and C. Du, *Mater. Sci. Eng., A*, 2017, **685**, 145–153.

50 D. D. Macdonald, *J. Supercritical Fluids*, 2004, **30**, 375–382.

51 J. Newman and K. E. Thomas-Alyea, *Electrochemical systems*, John Wiley & Sons, 2012.

52 D. Brazier and G. Freeman, *Can. J. Chem.*, 1969, **47**, 893–899.

53 S. Dahl, A. Logadottir, R. Egeberg, J. Larsen, I. Chorkendorff, E. Törnqvist and J. K. Nørskov, *Phys. Rev. Lett.*, 1999, **83**, 1814.

54 A. Cao, V. J. Bukas, V. Shadravan, Z. Wang, H. Li, J. Kibsgaard, I. Chorkendorff and J. K. Nørskov, *Nat. Commun.*, 2022, **13**, 2382.

55 B. Hammer and J. K. Norskov, *Nature*, 1995, **376**, 238–240.

56 R. Horne and D. Johnson, *J. Phys. Chem.*, 1967, **71**, 1147–1149.

57 S. Sawamura, Y. Yoshimura, K. Kitamura and Y. Taniguchi, *J. Phys. Chem.*, 1992, **96**, 5526–5529.

58 L. B. Sargent Jr, *ASLE Trans.*, 1983, **26**, 1–10.

59 J. Newman and N. P. Balsara, *Electrochemical systems*, John Wiley & Sons, 2021.

60 H. Saitoh, A. Machida and K. Aoki, *Chin. Sci. Bull.*, 2014, **59**, 5290–5301.

61 J. Valenta, T. Naka, M. Diviš, M. Vališka, P. Proschek, K. Vlášková, M. Klicpera, J. Prokleška, J. Custers and J. Prchal, *J. Phys.: Condens. Matter*, 2020, **32**, 425601.

62 S. Gabáni, M. Orendáč, J. Kušnír, E. Gažo, G. Pristáš, T. Mori and K. Flachbart, *J. Low Temp. Phys.*, 2017, **187**, 559–564.

63 Y. Lu, H. Kono, T. Larkin, A. Rost, T. Takayama, A. Boris, B. Keimer and H. Takagi, *Nat. Commun.*, 2017, **8**, 1–7.

64 T. Suski, J. Zulawnik and M. Malinowski, *J. Phys. E: Sci. Instrum.*, 1982, **15**, 1016.

65 Y. Han, S. Axnanda, E. J. Crumlin, R. Chang, B. Mao, Z. Hussain, P. N. Ross, Y. Li and Z. Liu, *J. Phys. Chem. B*, 2018, **122**, 666–671.

66 Y. Medina-Gonzalez, A. Jarray, S. Camy, J.-S. Condoret and V. Gerbaud, *J. Solution Chem.*, 2017, **46**, 259–280.

67 B. Li, C. Ji, W. Yang, J. Wang, K. Yang, R. Xu, W. Liu, Z. Cai, J. Chen and H.-K. Mao, *Proc. Natl. Acad. Sci. U. S. A.*, 2018, **115**, 1713–1717.

68 J. Philippe, Y. Le Godec, M. Mezouar, M. Berg, G. Bromiley, F. Bergame, J. Perrillat, M. Alvarez-Murga, M. Morand and R. Atwood, *High Press. Res.*, 2016, **36**, 512–532.

69 S. Li, Y. Zhou, K. Li, M. Saccoccio, R. Sažinas, S. Z. Andersen, J. B. Pedersen, X. Fu, V. Shadravan and D. Chakraborty, *Joule*, 2022, **6**, 2083–2101.

70 D. E. Garrett, *Chemical engineering economics*, Springer Science & Business Media, 2012.

71 C. M. Evans, M. R. Singh, N. A. Lynd and R. A. Segalman, *Macromolecules*, 2015, **48**, 3303–3309.